A NANOWIRE GAUGE FACTOR EXTRACTION METHOD FOR MATERIAL COMPARISON AND IN-LINE MONITORING

Issam Ouerghi, Julien Philippe, Carine Ladner, Pascal Scheiblin, Laurent Duraffourg, Sébastien Hentz and Thomas Ernst
CEA, LETI, MINATEC Campus, 17 rue des Martyrs - 38054 GRENOBLE Cedex 9, France

ABSTRACT

We propose a new non-destructive extraction method of gauge factor (GF) of nanowires (NW) for in-line monitoring of this parameter and piezoresistive material properties comparisons. Unlike destructive conventional techniques which also suffer from reproducibility issues, this method allows a direct measurement of the GF locally at the nanoscale and at the wafer level. GFs have been reliably measured on a wide range of silicon-based NEMS resonators with different designs, crystalline structures and doping levels. For monocrystalline devices, the extracted values are in good agreement with typical values obtained for NWs fabricated with well-controlled top-down processes. These values are also compared with polysilicon (polySi) NEMS, which look promising for low cost solutions.

INTRODUCTION

Since the fifties, monocrystalline silicon is well known and used for its strong piezoresistive properties. Silicon-based piezoresistive devices have been introduced in several sensing applications, such as pressure sensors, accelerometers, cantilever force sensors, inertial sensors and strain gauges [1]. Moreover, piezoresistivity is now commonly used in CMOS, known as substrate [2] induced- or process [3] induced-strain for mobility enhancement. The piezoresistive effect is quantified by a change in the electrical resistivity when a mechanical stress is applied. The relative resistance variation is proportional to the axial strain and is simply expressed as $\Delta R/R = \gamma \times \varepsilon$ where γ is the piezoresistive GF. This resistance variation is mainly modeled by the piezoresistive tensor which accounts for the modulation of holes and electrons effective masses under strain [4]. Commonly, a high GF value for p-type silicon is associated to a longitudinal stress following the [110] direction. In this case, equal opposite values are obtained for longitudinal and transverse piezoresistive coefficients [1].

Piezoresistive coefficients and associated GFs of a bulk material are usually extracted by the four-point bending measurement [5-6]. The sample should be cleaved ($2 \times 8\,\mathrm{cm}^2$ in our experimental apparatus for example) and placed on a support rod to be submitted to a tensile or a compressive strain. This technique is slow, destructive since the samples must be cleaved, and suffers from repeatability issues. These drawbacks make it impossible to process GF data statistically at the wafer level. Moreover, at the nanoscale (NEMS devices) the piezoresistance is subject to surface and or dimensional effect that may affect its value as recently evidenced by several authors, which make relevant a simple, non-destructive method to monitor this property. For instance, a giant piezoresistance effect demonstrated by [7] was attributed by interface effects [5] and not reproduced with well controlled top-down processing, as used in the following study [8].

In this study, we demonstrate a new method to extract the local longitudinal GF directly at the wafer level. To this end, NWs are embedded into a simple nanomechanical device which can be used for in-line testing during fabrication or co-integration of NEMS devices. The results are then compared with the conventional method and some reference values to validate this approach.

NEMS STRCUTURE AND FABRICATION

The GF-testing device design is inspired from a NEMS sensor for chemical or mass sensing applications [9-10], see Figure 1. In this work, the device is only used in DC mode to properly study NW gauges properties. Its fabrication process is summarized in Figure 2. The NEMS is structured from a Silicon On Insulator (SOI) wafer by etching the top silicon. The top silicon and the buried oxide layers thicknesses are respectively 160 and 400nm. Electrical wires and pads are made with aluminum silicide (AlSi) metallic layer. The structure is then released by vapor hydrofluoric acid (HF) etching. The NEMS structure consists of two suspended piezoresistive p-doped silicon NWs connected to a rigid-enough lever (a cantilever) in a symmetric bridge configuration. The lever is electrostatically actuated, which induces high axial stress in the two piezoresistive gauges thanks to a large lever arm.

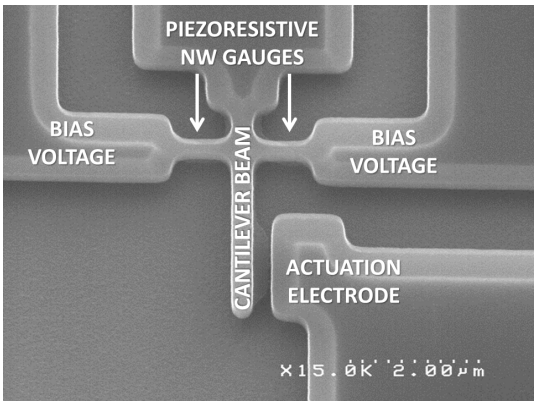

Figure 1: Top view SEM of the NEMS structure. Piezoresistive gauges are connected to a lever arm.

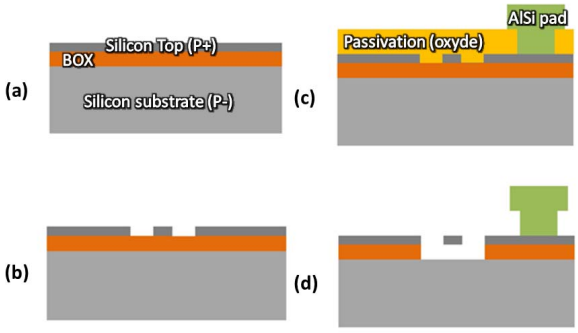

Figure 2: NEMS fabrication sequences: (a) Boron atoms implantation and activation, (b) Etching of the silicon top layer to define the NEMS (c) Passivation, metal deposition and etching for defining the metallic pads and (d) Release of the structure with a vapor HF to obtain suspended structure.

EXPERIMENT

With a van der Pauw method, we measured the resistivity of the layer before the NEMS fabrication step, therefore a nominal gauge resistance R_g of 1.5 kΩ was extracted. Considering the access resistances, this result is consistent with the electrical resistance measurement on the gauges. The maximum actuation voltage was fixed at 25 V before the collapse or the breakdown of the beam (experimentally we found a pull in voltage superior to 30 V). A low detection current through the gauges, below 100 µA, prevents from any actuation perturbation and avoids the NW gauges self-heating. The corresponding bias voltage is 250 mV. The gauge relative resistance is expected to vary with the DC actuation voltage applied to the electrode V_{act}. Indeed, the stress within one gauge can be expressed as $\sigma = \alpha_s \times E \times V_{act}^2$ where E is the Young's modulus of silicon and α_s is some transduction factor (in V^{-2}). Electromechanical Finite Element simulations were performed to obtain precise values of α_s (see Figure 3).

On the other hand, the relative piezoresistive gauge resistance variation is $\Delta R_g / R_g = \gamma \times \sigma / E$. Experimentally, resistance of a single gauge was monitored while varying V_{act}. Figure 4 shows the electrical current through the gauge and relative resistance variation with respect to the actuation voltage, a high signal-to-noise ratio is obtained thanks to the significant lever arm of this design. As expected, the relative resistance variation follows a quadratic law with the actuation voltage: $(\Delta R_g / R_g)_{\exp} = \alpha_e \times V_{act}^2$, where α_e is an experimental factor (in V^{-2}). Nevertheless, the proximity of the actuation electrode induces a linear field effect within the NWs, which adds up to the purely piezoresistive effect in the I-V curves shown in Figure 4(a)-(b). Poisson equations and continuity transport equations were solved numerically using an Arora mobility model [11] with a commercial TCAD tool (Silvaco's ATLASTM) to model the contribution of this effect (insets in Figure 4 (a)-(b)), yielding the simple equation: $I \approx 10^{-9} V_{act}$. This linear effect does not impact piezoresistive properties and can be subtracted from the I-V curves for GF extraction (Figure. 4 (c) and (d)). The device corresponds to a bridge configuration and the gauges feel an opposite stress for the same actuation voltage (applied on the same actuation electrode): the gauge resistance increases with the actuation voltage due to a tensile stress while the other gauge resistance decreases due to a compressive stress. These observations are consistent with others experiments for P-type silicon [5]. Finally, $\alpha_e = \gamma \times \alpha_s$ is plotted over α_s in Figure 5 for different device designs. The linear fit yields a GF value of 84 ± 2 for both tensile and compressive stresses.

DISCUSSIONS

In order to compare the experimental results with theoretical predictions, the theoretical GF value from the works of Richter et al [12] were analyzed. They used both a 6×6 $k \cdot p$ Hamiltonian and a tight binding model to predict the shear piezoresistive coefficient of p-type silicon according to both the dopant concentration and the temperature. At room temperature and for a doping level of 1×10^{19} cm^{-3}, they find a percentage of about 70 ± 5 % of the shear piezoresistive coefficient maximum value. That corresponds to other references [13] [14]. In the [110] direction, the maximum value (corresponding to a doping level $< 1 \times 10^{16}$ cm^{-3}) of the longitudinal piezoresistive coefficient π_l measured is 71.8×10^{-11} Pa^{-1} [15].

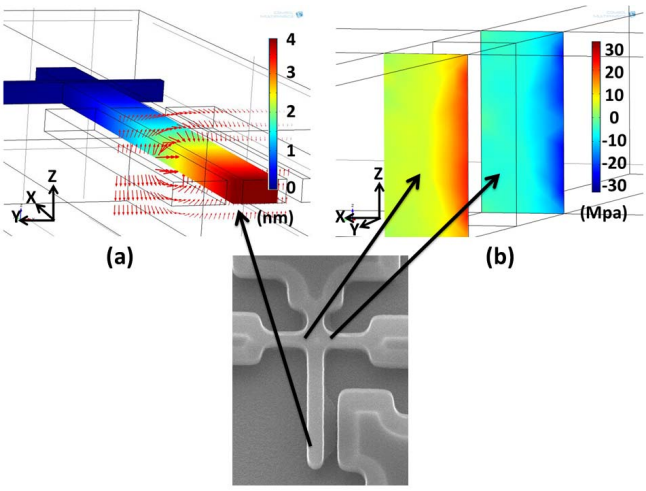

Figure 3: (Color) Electromechanical simulation of NEMS for an actuation voltage of 15 V. (a) The color legend and red arrows respectively represent the beam deflection and the electric field lines. (b) Simulated gauge stress on the surfaces between the gauges and the beam. Negative and positive values respectively represent a tensile and compressive stress. The average pressure on the surfaces is 8.0 MPa.

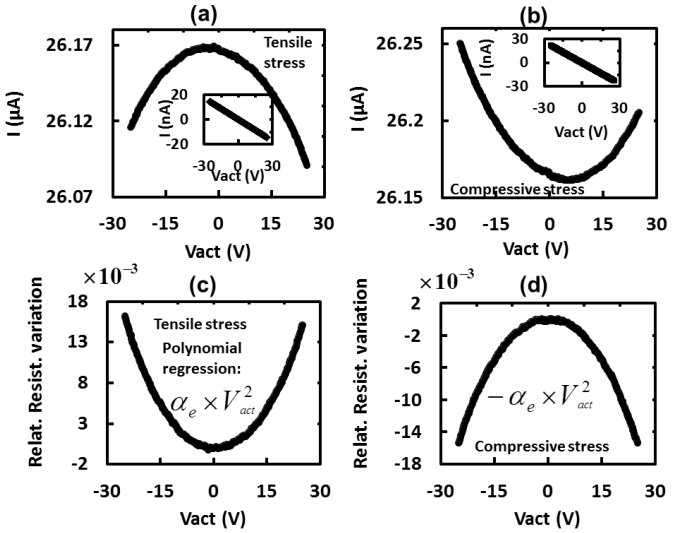

Figure 4: (a-b) I-V measurements of the gauge current versus the actuation voltage. The beam deflection involves a tensile stress on one gauge (a) and a compressive stress on the other (b). (c-d) Relative gauge resistance variations as a function of actuation voltage. A linear component of the current as a function of the actuation voltage (insets of (a) and (b)) due to a field effect between the gauges and the actuation electrode is suppressed.

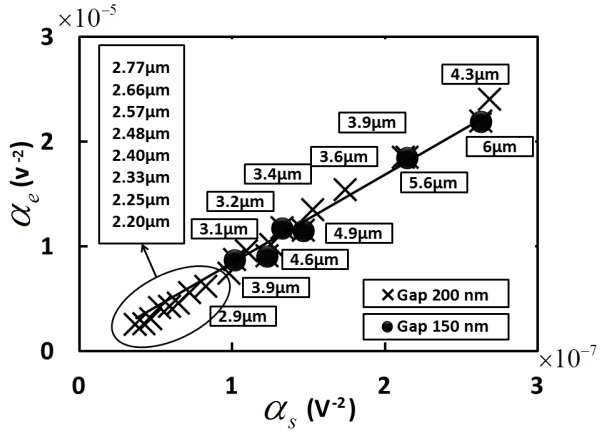

Figure 5: Comparison between simulation and experimental coefficients for different actuation-beam gaps and beam lengths. The linear fit gives directly the GF value.

Therefore the doping levels used in our experiments involves a theoretical GF value of $\gamma \approx \pi_l \times E \times 0.70 \pm 0.05 \approx 85 \pm 6$. Comparison of the GF values between our method and the four-point bending measurement was performed on rectangular-box-shaped devices ($3 \times 0.25 \times 0.25\,\mu m^3$). I-V measurements for each applied stress were performed to extract the resistance variation. As shown in Figure. 6, the GF is extracted thanks to the linear fit of the relative resistance variation as a function of strain curve and equal to 88 ± 4. This points out that our method is consistent with the conventional method and the expected theoretical value, i.e. 84 ± 2, 88 ± 4 and 85 ± 6 respectively. Giant piezoresistance effects [7] in suspended Si NWs have been quite widely studied these last years. This phenomenon does not concern highly doped top-down NW [8]. Moreover, the NW cross-section in this work is one order of magnitude larger than the NWs concerned by the giant piezoresistance effect. This characterization method could be extended on other piezoresistive materials providing the signal to noise ratio is sufficiently high. As example our method allowed for easy measurement of three different polySi NEMS GFs, briefly presented in Table 1.

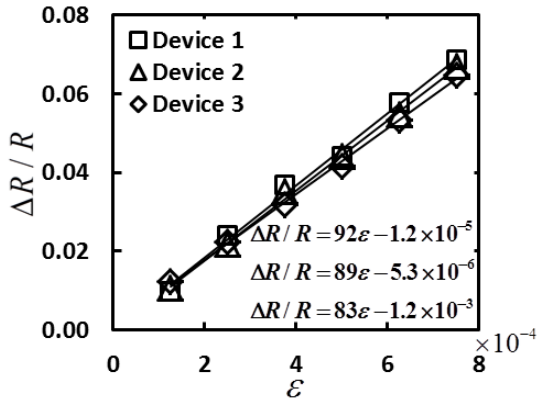

Figure 6: Four-point bending measurement performed on three devices (3×0.25×0.16 µm3) The linear fit gives directly the GF value.

Table 1. Comparison between extracted GFs with conventional and new method. Results are in good agreement. Unlike monocrystalline silicon, GF value for PolyB material increases with doping level.

	PolyA	PolyB		PolyC	Single crystal silicon	
Deposition conditions	0.175 Torr, 580° C	0.2 Torr, 620° C (columnar)		0.375 Torr, 580° C	SOI wafers	
Doping level	2.9×10^{20}cm^{-3}	10^{19} cm^{-3}	10^{20} cm^{-3}	7×10^{19}cm^{-3}	10^{19} cm^{-3}	10^{20} cm^{-3}
GF from conventional method	22	15	33	19	88	68
GF from the new method	**18**	**13**	**32**	**15**	**84**	**53**

CONCLUSIONS

In conclusion, a new characterization and extraction method of GF was presented. This design can be added as a test structure to monitor this parameter in parallel with other NEMS devices. Therefore it is fast enough to characterize a large number of NEMS at the wafer level and is hence compatible with NEMS VLSI. The results are consistent with theoretical data and with the conventional method and can be extended to other piezoresistive materials.

ACKNOWLEDGEMENTS

This work was supported by the European Research Council, Grant No. 240382 – DELPHINS project.

REFERENCES

[1] A. A. Barlian, W.-T. Park, A. J. R. Mallon, A. J. Rastegar, and B. L. Pruitt, "Review: Semiconductor Piezoresistance for Microsystems," *Proc. IEEE*, vol. 97, no. 3 Mar. 2009.

[2] F. Andrieu, O. Weber, T. Ernst, O. Faynot and S. Deleonibus, "Strain and channel engineering for fully depleted SOI MOSFETs towards the 32 nm technology node," *Microelectronic Engineering*, vol. 84, pp. 2047–2053, Sept.–Oct. 2007.

[3] F. Andrieu, T. Ernst, C. Ravit, M. Jurczak, G. Ghibaudo and S. Deleonibus, "In-Depth Characterization of the Hole Mobility in 50-nm Process-Induced Strained MOSFETs," *IEEE Electron Dev. Lett*., vol. 26, no. 10, Oct. 2005.

[4] J. Bardeen and W. Shockley, "Deformation Potentials and Mobilities in Non-Polar Crystals," *Phys. Rev.*, vol. 80, no. 1, Oct. 1950.

[5] A. Koumela, D. Mercier, C. Dupré, G. Jourdan, C. Marcoux, E. Ollier, S. T. Purcell, and L. Duraffourg, "Piezoresistance of top-down suspended Si nanowires," *J. Nanotechnology*, vol. 22, 395701, Sept. 2011.

[6] W.L Wang, X. Jiang, K. Taube and C. Klages "Piezoresistivity of polycrystalline p-type diamond films of various doping levels at different temperatures", *J. Appl. Phy.,* vol. 82, 2, 1997.

[7] R. He and P. Yang, "Giant piezoresistance effect in silicon nanowires," *nature nanotechnology*, vol. 1, pp. 42-46, Oct. 2006.

[8] J.S Milne and A.C.H. Rowe, "Giant Piezoresistance Effects in Silicon Nanowires and Microwires," *Phy. Rev. Lett.*, vol. 105, no. 22, Nov. 2010.

[9] M. S. Hanay, S. Kelber, A. K. Naik, D. Chi, S. Hentz, E. C. Bullard, E. Colinet, L. Duraffourg and M. L. Roukes, "Single-protein nanomechanical mass spectrometry in real time", *Nature Nanotechnology*, 7, pp. 602–608, 2012.

[10] E. Mile, G. Jourdan, I. Bargatin, S. Labarthe, C. Marcoux, P. Andreucci, S. Hentz, C. Kharrat, E. Colinet, and L. Duraffourg, "In-plane nanoelectromechanical resonators based on silicon nanowire piezoresistive detection," *Nanotechnology*, vol. 21, 165504, Mar. 2010.

[11] ND. Arora, JR. Hauser and DJ. Roulston, "Electron and Hole Mobilities in Silicon as a Function of Concentration and Temperature," *IEEE Trans. Electron Devices*, vol. 29, no. 2, Feb. 1982.

[12] J. Richter, J. Pedersen, M. Brandbyge, E. V. Thomsen, and O. Hansen, "Piezoresistance in p-type silicon revisited," *J. Appl. Phys.,* vol. 104, 023715, Jul. 2008.

[13] O. N. Tufte and E. L. Stelzer, "Piezoresistive Properties of Silicon Diffused Layers," *J. Appl. Phys*., vol. 34, pp. 313-318, Feb. 1963.

[14] Y. Kanda, "A Graphical Representation of the Piezoresistance Coefficients in Silicon," *IEEE Trans. Electron Devices*, vol. 29, pp. 64-70, Jan. 1982.

[15] C. S. Smith, "Piezoresistance Effect in Geruianium and Silicon," *Phys. Rev*., vol. 94, no. 1, pp. 42-49, Apr. 1954.

CONTACT

Thomas Ernst, Thomas.ernst@cea.fr